

Examination of Metal–Silicon Bonding through Structural and Theoretical Studies of an Isostructural Set of Five-Coordinate Silyl Complexes, $\text{Os}(\text{SiR}_3)\text{Cl}(\text{CO})(\text{PPh}_3)_2$ ($\text{R} = \text{F}, \text{Cl}, \text{OH}, \text{Me}$)

Klaus Hübler,* Patricia A. Hunt, Susan M. Maddock, Clifton E. F. Rickard, Warren R. Roper,* David M. Salter, Peter Schwerdtfeger, and L. James Wright

Department of Chemistry, The University of Auckland, Private Bag 92019, Auckland, New Zealand

Received July 9, 1997[®]

$\text{Os}(\text{SiCl}_3)\text{Cl}(\text{CO})(\text{PPh}_3)_2$ is prepared by treatment of $\text{OsPhCl}(\text{CO})(\text{PPh}_3)_2$ with excess HSiCl_3 and serves in turn as the starting material for the syntheses of three more five-coordinate silyl complexes $\text{Os}(\text{SiR}_3)\text{Cl}(\text{CO})(\text{PPh}_3)_2$ ($\text{R} = \text{F}, \text{OH}, \text{Me}$) via substitution of the chloride groups on silicon. All four compounds were fully characterized, including a single-crystal solid-state structure of each derivative. Carbonyl stretching frequencies decrease and Os–Si bond lengths increase as R changes in the order from F to Cl to OH to Me. *Ab initio* calculations were performed on the model complexes $\text{Os}(\text{SiR}_3)\text{Cl}(\text{CO})(\text{PPh}_3)_2$ ($\text{R} = \text{F}, \text{Cl}, \text{OH}, \text{Me}$) to explain the trends observed in the IR and X-ray studies, and the importance of the π -acceptor capacities of the silyl groups are discussed.

Introduction

A good understanding of the nature of the metal–silicon bond is important not only from a fundamental point of view but also for the development of successful catalysts for the production of an increasing range of organosilicon compounds. This understanding would give insight into elementary steps, such as the insertion of unsaturated molecules into M–Si bonds, which are of central importance for many catalytic processes.

Since the first synthesis of a compound with a M–Si bond in 1956,¹ there has been debate about the electronic nature of this linkage. Early recognition that some M–Si bond distances were conspicuously shorter than expected led to suggestions of a $d\pi$ – $d\pi$ contribution to the bonding. However, this view finds little current favor, and explanations involving increased ionic character to the bonding or explanations based on σ -effects alone (more s-character in the M–Si bond, more p-character in the Si–substituent bond) are more popular. A valuable photoelectron spectral study by Lichtenberger and Rai-Chaudhuri established that the trichlorosilyl ligand in $\text{CpFe}(\text{CO})_2\text{SiCl}_3$ is an effective π -acceptor.² These authors suggest that the π -back-bonding to SiCl_3 involves significant portions of the Si–Cl σ^* -orbitals. A related study³ of $\text{Co}(\text{CO})_4\text{SiCl}_3$, $\text{Mn}(\text{CO})_5\text{SiCl}_3$, and *cis*- $\text{Fe}(\text{CO})_4(\text{SiCl}_3)_2$ concludes that π -acceptance is not important here, but it should be noted that in each of these compounds all accompanying ligands are CO, a circumstance clearly unfavorable for π -acceptance by SiCl_3 .

One of the problems encountered in probing the nature of the M–Si bond by various physical techniques

has its origin in the lack of general synthetic procedures. It is not always possible to find a series of compounds, all closely related, in which there is a systematic variation of substituents on the silicon. The accessibility to us of a set of five-coordinate osmium–silyl complexes where the silyl ligand changes from SiF_3 to SiCl_3 to $\text{Si}(\text{OH})_3$ to SiMe_3 prompted us to collect a complete set of structural data from single-crystal X-ray diffraction studies and to complement these data with *ab initio* calculations. The conclusions from these studies are reported in this paper.

Results and Discussion

Syntheses. The five-coordinate silyl complexes were conveniently prepared in good yield from $\text{Os}(\text{SiCl}_3)\text{Cl}(\text{CO})(\text{PPh}_3)_2$ (**1b**) via substitution reactions involving the chloride groups on silicon. **1b** was in turn isolated as a yellow crystalline solid by treatment of $\text{OsPhCl}(\text{CO})(\text{PPh}_3)_2$ with excess HSiCl_3 in toluene at 40 °C for 30 min, Scheme 1. An attempt to synthesize the analogous trimethylsilyl derivative $\text{Os}(\text{SiMe}_3)\text{Cl}(\text{CO})(\text{PPh}_3)_2$ from $\text{OsPhCl}(\text{CO})(\text{PPh}_3)_2$ and HSiMe_3 failed. Instead, the reaction resulted in the production of the osmium(IV) product $\text{Os}(\text{SiMe}_3)_3\text{H}_3(\text{CO})(\text{PPh}_3)_2$.⁵ To obtain compound **1d**, $\text{Os}(\text{SiCl}_3)\text{Cl}(\text{CO})(\text{PPh}_3)_2$ was treated with methyl-lithium at room temperature in toluene. A color change from yellow to red-orange occurred, and $\text{Os}(\text{SiMe}_3)\text{Cl}(\text{CO})(\text{PPh}_3)_2$ (**1d**) was isolated as a yellow-orange solid.

A convenient route to the fluorosilyl derivative **1a** involved reaction of either $\text{Os}[\text{Si}(\text{OH})_3]\text{Cl}(\text{CO})(\text{PPh}_3)_2$ ⁶ or $\text{Os}[\text{Si}(\text{OEt})_3]\text{Cl}(\text{CO})(\text{PPh}_3)_2$ ⁷ with aqueous HF at room temperature for a short time. **1a** is relatively unreactive

[®] Abstract published in *Advance ACS Abstracts*, October 15, 1997.

(1) Piper, T. S.; Lemal, D.; Wilkinson G. *Naturwissenschaften* **1956**, *43*, 129.

(2) Lichtenberger, D. L.; Rai-Chaudhuri, A. *J. Am. Chem. Soc.* **1991**, *113*, 2923.

(3) Novak, I.; Huang, W.; Luo, L.; Huang, H. H.; Ang, H. G.; Zybill, C. E. *Organometallics* **1997**, *16*, 1567.

(4) Rickard, C. E. F.; Roper, W. R.; Taylor, G. E. J.; Waters, M.; Wright, L. J. *J. Organomet. Chem.* **1990**, *389*, 375.

(5) Details of this compound will be reported elsewhere.

(6) Rickard, C. E. F.; Roper, W. R.; Salter, D. M.; Wright, L. J. *J. Am. Chem. Soc.* **1992**, *114*, 9682.

(7) Maddock, S. M. Thesis, The University of Auckland, Auckland, New Zealand, 1995.

Scheme 1

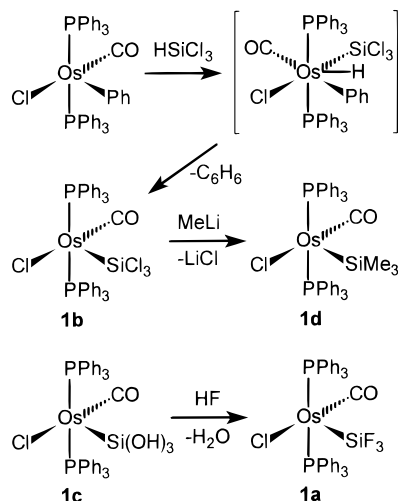


Table 1. C–O Stretching Frequencies (cm⁻¹) for Compounds of the Type Os(SiMe_{3-n}R_n)Cl(CO)-(PPh₃)₂ (R = F, Cl, OH; n = 0–3)

	F	Cl	OH
SiMe ₃	1895	1895	1895
SiMe ₂ R	1917 ⁷	1917 ⁸	1910 ⁸
SiMeR ₂	1933 ⁷	1928 ⁸	1917 ⁸
SiR ₃	1946	1944	1919

and can be recrystallized from dichloromethane/ethanol without alcoholysis occurring.

IR Spectra. The $\nu(\text{CO})$ absorptions of solid samples of compounds **1a** and **1d** were split into two bands, which collapsed to one single peak each when the spectra were recorded as dichloromethane solutions, suggesting solid-state splitting. The $\nu(\text{CO})$ values of the isostructural set of five-coordinate silyl complexes with the formula $\text{Os}(\text{SiMe}_{3-n}\text{R}_n)\text{Cl}(\text{CO})(\text{PPh}_3)_2$ (R = F,⁷ Cl,^{6,8} OH;^{6,8} n = 0–3) are listed in Table 1. The $\nu(\text{SiF})$ values for compound **1a** are found between 880 and 820 cm⁻¹, and $\nu(\text{SiCl})$ for compound **1b** are hidden by absorption bands of the triphenylphosphine ligands.

Examination of Table 1 shows that sequential replacement of the Me groups in $\text{Os}(\text{SiMe}_3)\text{Cl}(\text{CO})(\text{PPh}_3)_2$ with either OH, Cl, or F causes the $\nu(\text{CO})$ values to increase. Furthermore, the magnitude of this effect depends on the substituents in the order F > Cl > OH. There appears to be a correlation between the electronegativity of the silyl group and the position of $\nu(\text{CO})$. The electronegativity of a silyl group can be estimated by theoretical methods and is dependent upon the substituents attached to silicon and the method used.⁹ For the complexes in this study, the silyl group with the highest group electronegativity is clearly SiF₃, the SiMe₃ group has the lowest electronegativity.

A shift of the carbonyl stretching frequency $\nu(\text{CO})$ to higher wavenumbers is usually explained by a decrease of the electron density on the metal available for π -backbonding to the $\pi^*(\text{CO})$ -orbitals. This decrease may be due to an increase in the π -accepting capacity (–M) or only due to a simple inductive σ -withdrawing effect (–I) of the silyl group as more electronegative substituents are placed on silicon. The importance of these two

Table 2. Crystallographic Data for Os(SiR₃)Cl(CO)(PPh₃)₂ with R = F, Cl, and Me

	R = F (1a)	R = Cl (1b)	R = CH ₃ (1d)
formula	C ₃₇ H ₃₀ ClF ₃ OOSiP ₂	C ₃₈ H ₃₀ Cl ₂ OOSiP ₂	C ₄₀ H ₃₉ ClOOSiP ₂
fw	863.29	995.55	851.39
a, pm	1365.9(4)	1029.2(3)	1162.78(8)
b, pm	1234.2(4)	1997.4(4)	1879.9(2)
c, pm	2022.7(6)	1969.2(2)	1697.9(3)
β , (deg)	97.57(3)	91.370(10)	96.181(9)
V, m ³	3380(2) × 10 ⁻³⁰	4047(2) × 10 ⁻³⁰	3689.9(8) × 10 ⁻³⁰
Z	4	4	4
space group	P2 ₁ /c	P2 ₁ /n	P2 ₁ /c
T, °C	20	20	20
λ , pm	71.069	71.069	71.069
ρ_{calc} , g cm ⁻³	1.696	1.634	1.533
μ , mm ⁻¹	4.03	3.68	3.68
R (F _o) ^a	0.0341	0.0332	0.0335
R _w (F _o ²) ^a	0.0793	0.0829	0.0757
S	1.096	1.053	1.075

^a $R(F_o) = \sum ||F_o| - |F_c|| / \sum |F_o|$. $R_w(F_o^2) = \{\sum [w(F_o^2 - F_c^2)^2] / \sum [w(F_o^2)^2]\}^{1/2}$.

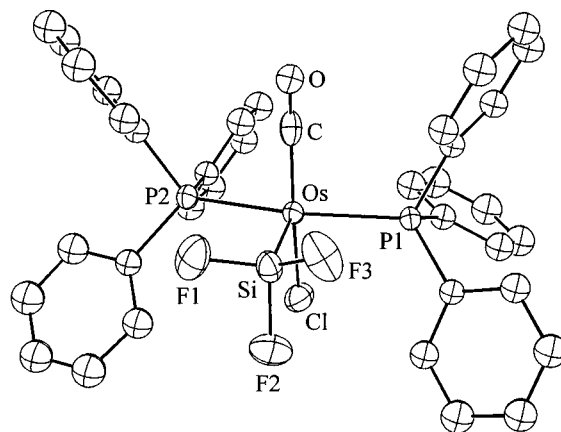


Figure 1. Molecular structure of $\text{Os}(\text{SiF}_3)\text{Cl}(\text{CO})(\text{PPh}_3)_2$ (**1a**). All hydrogen atoms are omitted for clarity.

effects on the carbonyl stretching frequency will be discussed in the following sections.

X-ray Structures of Compounds 1a–d. Crystals of $\text{Os}(\text{SiF}_3)\text{Cl}(\text{CO})(\text{PPh}_3)_2$ (**1a**), $\text{Os}(\text{SiCl}_3)\text{Cl}(\text{CO})(\text{PPh}_3)_2$ (**1b**), and $\text{Os}(\text{SiMe}_3)\text{Cl}(\text{CO})(\text{PPh}_3)_2$ (**1d**) suitable for single-crystal X-ray structure determination were grown from dichloromethane/ethanol, toluene/*n*-hexane, and benzene/diethyl ether mixtures, respectively. Crystal data and data collection parameters are listed in Table 2. Although the structure of $\text{Os}[\text{Si}(\text{OH})_3]\text{Cl}(\text{CO})(\text{PPh}_3)_2$ (**1c**) has already been published,⁶ this compound will also be discussed because of the close relationship with the other three complexes reported here for the first time.

The largest angles around osmium are P–Os–P (166.55(6)°, 163.3(2)°, 165.8(1)°, 158.97(5)°) and Cl–Os–C (167.0(2)°, 165.3(14)°, 168.9(2)°, 170.9(4)°) for **1a–d** respectively, and in each case the four angles involving Si and Os are all close to 90°. Thus, compounds **1a–d** all have a similar geometry which can be described as square pyramidal with the silyl group, which has the largest *trans* influence, in the apical position. Therefore, the structure of only one of these compounds, $\text{Os}(\text{SiF}_3)\text{Cl}(\text{CO})(\text{PPh}_3)_2$ (**1a**) is depicted in Figure 1. The difference in the orientation of the silyl substituents with respect to the basal plane ligands in the four structures **1a–d** can be conveniently described by the torsion angle Cl–Os–Si–R_i which has values of 5.6(3)°, –8.2(5)°, 14.4(2)°, and –2.6(3)° for the trifluo-

(8) Salter, D. M. Thesis, The University of Auckland, Auckland, New Zealand, 1993.

(9) Huheey, J. E. *J. Phys. Chem.* **1965**, *69*, 3284

Table 3. Selected Interatomic Distances (pm) and Angles (deg) for Os(SiR₃)Cl(CO)(PPh₃)₂ and the Model Compounds Os(SiR₃)Cl(CO)(PH₃)₂ (a–d, R = F, Cl, OH, Me)

compound method	1a, X-ray	2a, BLYP	1b, X-ray	2b, BLYP	1c, X-ray	2c, BLYP	1d, X-ray	2d, BLYP
Os–Si	225.4(2)	231.2	227.3(6)	232.0	231.9(2)	237.0	237.4(2)	242.7
Si–R _i ^a	159.5(5)	162.7	206.1(10)	212.0	164.9(5)	164.0	189.9(8)	190.0
Si–R _o ^{a,b}	156.7(5)	163.1	205.9(8)	212.9	164.7(5)	167.5	186.6(7)	190.1
	156.1(5)		206.9(9)		162.4(5)		189.0(7)	
Os–Cl ^c	240.0(2)	247.8	243.5(13)	248.0	241.9(2)	249.1	244.7(4)	250.8
Os–C ^c	189.2(8)	186.5	187 (4)	186.4	188.5(9)	185.3	175.5(13)	185.5
C–O ^c	103.1(8)	121.1	104 (4)	121.0	100.5	122.1	117.1(14)	121.9
Os–P ^b	238.4(2)	245.0	237.7(5)	245.6	238.1(1)	244.0	237.9(1)	243.3
	237.0(2)		240.3(5)		236.2(1)		236.3(1)	
Os–Si–R _i ^a	113.6(2)	113.0	116.5(3)	109.8	111.3(2)	108.5	112.3(3)	108.1
Os–Si–R _o ^{a,b}	117.9(2)	115.4	115.7(3)	116.1	115.6(2)	113.7	114.9(2)	113.6
	118.0(2)	118.5(4)		113.9(2)		114.9(2)		
R _i –Si–R _o ^{a,b}	99.4(3)	103.6	103.1(4)	104.6	102.8(3)	105.6	104.9(4)	107.8
	100.3(3)		100.8(5)		106.4(4)		105.8(4)	
R _o –Si–R _o ^a	104.8(3)	104.5	99.5(4)	104.3	105.9(4)	109.0	103.1(4)	105.7
Si–Os–C ^c	89.2(2)	85.8	93.0(13)	86.4	86.4(2)	84.6	88.6(4)	86.7
Si–Os–Cl ^c	103.8(9)	114.3	101.6(3)	119.3	104.6(1)	114.9	100.46(11)	107.9
Si–Os–P ^b	94.48(6)	92.4	98.3(2)	93.7	94.7(1)	91.4	98.94(5)	94.1
	98.93(7)		98.4(2)		99.6(1)		102.02(5)	
Cl–Os–C(O) ^c	167.0(2)	159.8	165.3(14)	154.3	168.9(2)	160.5	170.9(4)	165.4
P–Os–P	166.55(6)	170.9	163.3(2)	169.2	165.8(1)	169.5	158.97(5)	168.7
Cl–Os–Si–R _i	5.6(3)	0.0	–8.2(5)	–0.1	14.4(2)	0.0	–2.6(3)	0.0

^a The index i stands for *in* plane (*C*₃) and the index o for *out* of plane. For the X-ray structures, R_i is R2, R_o is R1 and R3 (R = F, Cl, O, C). ^b For the X-ray data of compounds **1a–d**, the bond lengths and angles for R1 and P1 are listed first, followed by the values for R3 and P2. The calculated structures have almost perfect *C*₃ symmetry, and thus only an averaged parameter is listed. ^c For the disordered structures **1b** and **1d**, only the parameters for the isomer analogous to the fluorine derivative depicted in Figure 1 are given.

rosilyl, trichloro, trihydroxy, and trimethyl derivatives, respectively. While the triphenylphosphine and chloride ligands are always bent away from the silyl group with angles considerably exceeding 90° (94.48(6)–102.02(5)°), the Si–Os–C angle is always the smallest from the apical silicon to any of the equatorial ligands (86.4(2)–93.0(13)°). Disorder was found in the crystallographic unit cell for the chloride and carbonyl ligands in the complexes **1b** and **1d**, preventing the exact positions of these ligands from being determined. The structures were refined using the disorder model with a weighting of 50% occupancy for the atoms of the Cl and CO groups in the possible orientations. Selected bond lengths and angles are tabulated in Table 3. For the disordered structures **1b** and **1d**, only the parameters for the isomer analogous to the fluorine derivative depicted in Figure 1 are given.

The Os–Cl (240.0(2)–244.7(4) pm) and Os–P bond lengths (236.2(1)–240.3(5) pm) are very similar in all derivatives and fall within the range observed for a variety of osmium compounds (standard values, Os–Cl = 238.0 pm for 393 and Os–P = 238.4 pm for 236 observations).¹⁰ In general, the Os–Si bond becomes shorter as groups of greater electronegativity are placed on silicon. This phenomenon has been observed for other transition-metal–silyl complexes. To our knowledge, the Os–Si bond length of 225.4(2) pm for compound **1a** is the shortest Os–Si bond length so far reported. We note that the bond lengths of 227.3(6) and 231.9(2) pm for the trichloro and trihydroxy derivatives are shorter than that reported for a base-stabilized osmium silylene complex, Os{=SiEt₂(thf)}(thf)(TTP) (TTP = the dianion of tetra-*p*-tolylporphyrin, thf = tetrahydrofuran), of 232.5(8) pm.¹¹ The Os–Si distance in the trimethylsilyl derivative **1d** is 237.4(2) pm. It is

noteworthy that even this value is still much shorter than the Os–Si single bond distance of 250 pm,¹² which is predicted from the sum of the covalent radii of Os and Si.

The shorter Os–Si bond lengths observed when more electronegative groups are placed on silicon would be consistent with increasing the π -bonding from the metal to the silyl group. This would cause π -bonding to CO to decrease, the Os–C bond distance to lengthen, and the CO bond to contract. Although the ν (CO) values show the expected increase going from the trimethylsilyl to the trifluorosilyl compound (see Table 1), a discussion of the trends in Os–C bond lengths is complicated by the Cl/CO disorder in compounds **1b** and **1d**. Since any effects due to multiple bonding between osmium and silicon should be most obvious for Os(SiF₃)Cl(CO)(PPh₃)₂ (**1a**) with the highly electronegative fluoro substituents attached to silicon, the structure of **1a** will be discussed in more depth. Fortunately, the structure of **1a** is not subject to any disorder.

In addition to a very short Os–Si bond length in **1a**, the bond angles around silicon are distorted from a tetrahedral geometry and the average Os–Si–F bond angle is 116.5°. The Os–Si–F₂ angle of 113.6(2)° is significantly different from the other two of 118.0(2)° and 117.9(2)°. The average F–Si–F angle is 101.5°. These distortions around silicon are characteristic of silyl ligands with electron withdrawing groups on silicon. Bent's rule¹³ states that as some substituents on a central atom become more electronegative, increasing amounts of s-character are diverted to the orbitals used for bonding with the more electropositive substituents. In this case, this is the transition metal fragment OsCl(CO)(PPh₃)₂, and this may be an additional factor serving to decrease the Os–Si bond length. The larger p-character expected for the Si–F bonds results in a

(10) Allen, F. H.; Kennard, O. 3D Search and Research Using the Cambridge Structural Database. *Chemical Design Automation News* **1993**, 8, 1, 31.

(11) Woo, L. K.; Smith, D. A.; Young, V. G., Jr. *Organometallics* **1991**, 10, 3977.

(12) Pauling, L. *The Nature of the Chemical Bond*, 3rd ed.; Cornell University Press: Ithaca, New York, 1960.

(13) Bent, H. A. *Chem. Rev.* **1961**, 61, 275.

decrease of the F–Si–F angles from the ideal tetrahedral angle of 109.5°.

One Si–F bond (Si–F2, bond length of 159.5(5) pm) is significantly longer than the other two of 156.7(5) and 156.1(5) pm. The Si–F bond length in HSiF₃ is 156.1(5) pm.¹⁴ In Ni(SiF₃)₂(PMe₃)₃, where the only potential π -acceptor ligands are SiF₃, the average bond lengths for the two sets of three Si–F bonds are longer at 159.6(9) and 158.0(8) pm.¹⁵ This is consistent with π -bond formation between Ni and Si involving the Si–F σ^* -orbitals. The variation in the Si–F bond lengths observed in Os(SiF₃)Cl(CO)(PPh₃)₂ suggests that one Si–F σ^* -orbital may be more heavily involved in bond formation to Os than the other two.

Because of the Cl/CO disorder problem in each of the complexes **1b** and **1d**, it is not reasonable to expect observable differentiation between the Si–R distances for these compounds. The trihydroxysilyl derivative **1c**, which is not disordered, also has one silyl substituent (O2) arranged nearly *trans* to the carbonyl ligand with a torsion angle Cl–Os–Si–O2 of 14.4(2)°. However, there are no significant differences between the three Si–O distances found in **1c**.

The Si–Cl bonds of Os(SiCl₃)Cl(CO)(PPh₃)₂ were found to be 205.9(8), 206.1(10) and 206.9(9) pm and these are significantly longer than the average of 202 pm found for Si–Cl bond lengths in chlorosilane molecules.¹⁶ Similarly, long Si–Cl distances of 206.7, 206.9, and 207.2 pm were found in CpFe(SiCl₃)(CO)₂,¹⁷ for which some multiple bond between silicon and iron was proposed through photoelectron spectroscopy.² It is, therefore, possible that some degree of multiple bonding may be present in the Os–Si bond of **1b**. In contrast, the Si–C bond lengths of the SiMe₃ group in Os(SiMe₃)Cl(CO)(PPh₃)₂ (average 188.5 pm) appear normal.

The average angles R–Si–R and Os–Si–R on going from **1a–d** are found to be 101.5°, 101.1°, 105.0°, 104.6° and 116.5°, 116.9°, 113.6°, 114.0°, respectively. Although the general trends are in the direction expected from application of Bent's rule, the changes are very small and not uniform throughout this series of compounds. It is also difficult to predict the relative influence that steric factors have on these parameters.

Ab Initio Calculations. Model complexes Os(SiR₃)Cl(CO)(PH₃)₂ (**2a–d**; R = F, Cl, OH, Me) were constructed following the usual practice of replacing the bulky triphenylphosphine groups by PH₃, recognizing that the Os–P bond lengths will be underestimated. Geometry optimizations were performed on each of the four model compounds as well as on the parent silanes HSiR₃ (**3a–d**; R = F, Cl, OH, Me). A comparison with the experimentally obtained data for the transition metal complexes is shown in Table 3. The results of the calculations on the free silanes **3a–d** are listed in Table 4. The agreement between calculated and observed structures is generally good regarding the level of approximation used and the fact that solid-state effects are neglected. The results are certainly sufficiently good for the discussion of bond properties and

Table 4. Results of the Geometry Optimization and NBO Analyses for the Silanes HSiR₃ (R = F, Cl, OH, Me)^a

	3a (R = F)	3b (R = Cl)	3c (R = OH)	3d (R = Me)
H–Si	145.7	146.3	145.5	148.7
Si–R	160.2	207.6	164.2	188.8
H–Si–R	110.7	109.1	106.5	108.3
R–Si–R	108.3	109.9	112.3	110.6
<i>q</i> _H	–0.29	–0.19	–0.28	–0.24
<i>q</i> _{Si}	2.21	1.23	2.15	1.55
<i>q</i> _R	–0.64	–0.35	–0.62	–0.44
pop(3s _{Si})	0.68	0.97	0.64	0.79
pop(3p _{Si})	1.04	1.73	1.15	1.63
pop(3d _{Si})	0.07	0.07	0.06	0.03
BO(H–Si)	0.70	0.80	0.69	0.74
BO(Si–R)	0.34	0.61	0.26	0.55
3 R → Si	16.4%	19.7%	16.4%	3.3%

^a Interatomic distances (pm) and angles (deg), charges *q*, populations (pop), and atom–atom net linear bond orders (BO) based on the NLMO/NPA.³⁰

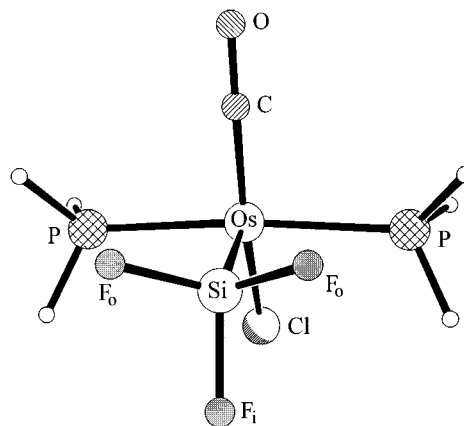


Figure 2. BLYP optimized structure of Os(SiF₃)Cl(CO)(PH₃)₂ (**2a**).

trends. In the following discussion, the term *in plane* (as opposed to *out of plane*) is used for atoms or orbitals which are part of the mirror plane (*C_s* symmetry) of the molecule. Technical details relating to the calculations can be found under Computational Details in the Experimental Section.

A simple comparison between Figures 1 and 2 shows that the calculated complexes **2a–d** have the same conformation as the structures **1a–d** obtained by X-ray crystallography. With no influence from packing effects, the structures of the computed species **2a–d** show perfect *C_s* symmetry with one substituent on silicon located exactly *trans* to the carbonyl group on osmium. In the following discussion, most of the trends in bond angles and distances occur when the substituents on silicon change in the order fluorine to chlorine to hydroxy to methyl. However, the group electronegativities of the different SiR₃ ligands with or without taking into account the calculated charges for those fragments shows the following descending values: SiF₃ (3.35 or 3.47) > Si(OH)₃ (3.01 or 3.10) > SiCl₃ (2.78 or 2.76) > SiMe₃ (2.27 or 2.30).⁹ This correlates with the order of the electronegativities of the substituents on silicon itself with F (3.89) > OH (3.22) > Cl (2.95) > Me (2.27).⁹ However, chlorine is similar in size to silicon and, therefore, forms covalent bonds more readily with this element than the other three substituents. Thus, only comparison of the different electronegativities of the second period elements are unambiguous.

(14) Eaborn, C. *Organosilicon Compounds*; Butterworths Scientific Publications: London, 1960.

(15) Bierschenk, T. R.; Guerra, M. A.; Juhlke, T. J.; Larson, S. B.; Lagow, R. J. *J. Am. Chem. Soc.* **1987**, *109*, 4855.

(16) Jolly, W. L. *The Principles of Inorganic Chemistry*; McGraw-Hill: New York, 1976; p 33.

(17) Schubert, U.; Kraft, G.; Walther, E. Z. *Anorg. Allg. Chem.* **1984**, *519*, 96.

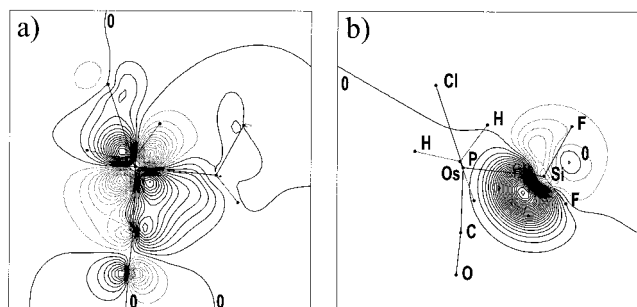


Figure 3. (a) Contour plot of the natural localized molecular orbital (NLMO) for the delocalization of the lone pair lp_1 on osmium for $Os(SiF_3)Cl(CO)(PH_3)_2$ (**2a**) generated with the program MOLDEN.³³ (b) Contribution of silicon orbitals to this NLMO. Full lines designate positive and dotted lines designate negative values of the orbital changing in steps of 0.02 for part a and 0.002 for part b.

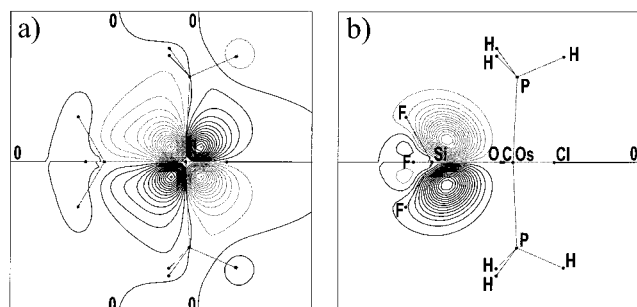


Figure 4. Contour plots for the delocalization of the lone pair lp_0 on osmium for $Os(SiF_3)Cl(CO)(PH_3)_2$ (**2a**) analogous to those shown in Figure 3.

Figures 3a and 4a show in-plane and out-of-plane electron isodensity contour maps for the delocalization of the lone pairs on osmium of complex **1a**. Figures 3b and 4b depict the contributions of silicon orbitals to the NLMOs in the corresponding parts a. Table 5 summarizes the results for the NBO analyses of **1a–d**. Comparable parameters of the NBO analyses for the free silanes **3a–d** are listed in Table 4.

Most of the calculated bond distances in the model compounds **2a–d** are longer than the parameters obtained from the X-ray data (see Experimental Section, Computational Methods), but they show the same trends that were found in the solid-state structures **1a–d**. The Os–Si distances, for example, are consistently overestimated by 5–6 pm in the BLYP calculations and change from 231.2 (**2a**) to 232.0 (**2b**), 237.0 (**2c**), and 242.7 pm (**2d**). These changes in bond lengths correlate partly with the difference between the electronegativity of the osmium fragment and the silyl group, $\Delta EN(OsSi)$, and this raises the question of the importance of ionic contributions in determining the length of the Os–Si bond. Since the charge on osmium in the complexes **2a–d** is almost invariant, the electronegativity of the osmium fragment can be considered to be approximately the same in all complexes and most likely to be smaller than 2.3, the value calculated for the trimethylsilyl compound **2d**. Since the group electronegativity of SiF_3 is larger by 1.17 than the value for $SiMe_3$, $\Delta EN(OsSi)$ also increases by 1.17 when going from the trimethylsilyl (**2d**) to the trifluorosilyl derivative (**2a**). According to Schomaker and Stevenson, an increase of 1.17 units in ΔEN is related to a shortening of approximately 10.5 pm in the corresponding bond in the absence of multiple

Table 5. Results of the NBO Analyses for the Model Complexes $Os(SiR_3)Cl(CO)(PH_3)_2$ (2a–d**)^{a,b}**

compound	2a (R = F)	2b (R = Cl)	2c (R = OH)	2d (R = Me)
q_{Os}	−0.43	−0.35	−0.40	−0.38
q_{Si}	2.08	1.08	2.09	1.59
q_{R1}^c	−0.65	−0.35	−0.62	−0.44
q_{R0}^c	−0.66	−0.38	−0.64	−0.47
q_{SiR3}	0.11	−0.03	0.19	0.21
q_{Cl}	−0.47	−0.46	−0.49	−0.51
q_C	0.41	0.43	0.38	0.42
q_O	−0.46	−0.46	−0.51	−0.50
q_P	0.26	0.27	0.27	0.28
EN_R	3.89	2.95	3.22	2.27
EN_{SiR3}	3.35	2.78	3.01	2.27
$EN_{SiR3}(q_{SiR3})$	3.47	2.76	3.10	2.30
$pop(3s_{Si})$	0.73	1.04	0.67	0.82
$pop(3p_{Si})$	1.11	1.81	1.17	1.54
$pop(3d_{Si})$	0.07	0.06	0.06	0.03
$BO(Os-Si)$	0.79	0.94	0.73	0.71
$BO(Os-Cl)$	0.35	0.32	0.25	0.23
$BO(Os-C)$	1.19	1.20	1.40	1.40
$BO(Os-P)$	0.52	0.53	0.50	0.51
$BO(Si-R_1)^c$	0.32	0.57	0.35	0.53
$BO(Si-R_0)^c$	0.31	0.56	0.34	0.52
$BO(C-O)$	1.44	1.44	1.43	1.43
$BO(Si-Cl)$	0.09	0.10	0.05	0.05
$BO(Si-CO)$	0.16	0.14	0.11	0.10
$BO(Si-P)$	0.05	0.05	0.05	0.05
$lp_1(Os) \rightarrow Si^c$	4.8%	2.4%	1.6%	1.1%
$lp_0(Os) \rightarrow Si^c$	1.9%	2.5%	1.1%	0.5%
$lp_1(Os) \rightarrow C(O)^c$	14.6%	13.7%	10.7%	7.1%
3 R \rightarrow Si	16.2%	19.0%	15.9%	4.2%

^a Charges q and populations (pop).³⁰ Electronegativities (EN) on the Pauling scale are calculated according to literature.⁹

^b Atom–atom net linear bond orders (BO) and delocalization of the lone pairs on osmium as well as of the lone pairs (lp) and bonds of the R groups based on the NLMO/NPA analyses.³⁰ ^c The index i stands for *in* plane (C_s) and the index o for *out* of plane.

bonding or rehybridization.¹⁸ Ionic contributions would, hence, explain the Os–Si bond shortening of 11.5 pm when comparing **2a** (231.2 pm) with **2d** (242.7 pm). On the other hand, it is surprising that the calculated Os–Si bond length in $Os(SiCl_3)Cl(CO)(PPh_3)_2$ is almost as short as that in $Os(SiF_3)Cl(CO)(PPh_3)_2$ and much shorter than that in $Os[Si(OH)_3]Cl(CO)(PPh_3)_2$, although the group electronegativity of $SiCl_3$ (2.76) is much smaller than those of SiF_3 (3.47) and $Si(OH)_3$ (3.10). This clearly shows that factors other than ionic contributions alone have to be considered to explain the differences in the Os–Si distances in the set of five-coordinate silyl complexes **2a–d**.

As the Os–Si distances become shorter on changing the nature of R, a corresponding lengthening of the Si–R bonds also occurs. The average Si–R values for the calculated complexes are found to be 2.8 (**2a**), 5.0 (**2b**), 2.1 (**2c**), and 1.3 pm (**2d**) longer than those obtained from optimizations on the corresponding free silanes **3a–d**. When considering only the second row derivatives **2a**, **2c**, and **2d**, the largest effect is observed for the trifluorosilyl compound, the complex with the highest group electronegativity for the silyl substituent, and gets smaller with decreasing electronegativities. However, the lengthening of 5.0 pm for the Si–Cl bond in **2b** is much larger than those observed for the second period analogues. This is due to both the larger value of the Si–Cl bond length compared to the other Si–R (R = F, OH, Me) bonds and the fact that the Si–Cl bond in $HSiCl_3$ (**3b**) is in turn relatively short. This arises because of a higher back-bonding from chlorine to silicon

(18) Douglas, B.; McDaniel, D. H.; Alexander, J. J. *Concepts and Models of Inorganic Chemistry*, 2nd ed.; Wiley: New York, 1983; p 78.

(19.6%) when compared with the much smaller values for the delocalization of the lone pairs of fluorine (16.4%) and hydroxy (16.4%) in HSiF₃ (**3a**) and HSi(OH)₃ (**3c**), respectively. This effect partly reverses the electron-withdrawing effect of the electronegative chlorine atoms and, therefore, also explains the lowest charge on silicon of only +1.23 and +1.08 in both the free silane HSiCl₃ (**3b**) and the trichlorosilyl complex Os(SiCl₃)Cl(CO)-(PPh₃)₂ (**2b**), respectively.

Another frequently discussed feature in this context are the bond angles on silicon. According to Bent's rule, smaller angles are found between substituents with higher electronegativity, and this results in a larger s-character for the orbital pointing toward an electro-positive atom and, therefore, a shorter bond distance to this atom.¹³ Since the group electronegativities of Si(OH)₃ (3.10) and SiMe₃ differ by as much as 0.80 units, and the average Os–Si–R angles are almost invariant with values of 112.0° and 111.8°, respectively, this criterion is not applicable at least for the complexes **2a–d** discussed here.

As a further explanation, the particularly short Os–Si distances in **2a** and **2b** can also be attributed to multiple bonding between these two centers. Multiple bonding can most easily arise through interaction of the osmium d-orbitals with either the silicon d-orbitals or a suitable combination of σ^* -orbitals of the SiR₃ group. The two lone pairs on osmium, in plane (lp_i (Os)) and out of plane (lp_o (Os)) with respect to the C_s -symmetry of the molecule, delocalize into hybrids on silicon by 4.8% (**2a**, Figure 3), 2.4% (**2b**), 1.6% (**2c**), and 1.1% (**2d**) as well as 1.9% (**2a**, Figure 4), 2.5% (**2b**), 1.1% (**2c**), and 0.5% (**2d**), respectively, while the donation into the carbonyl π^* -orbitals of 14.6% (**2a**, Figure 3a), 13.7% (**2b**), 10.7% (**2c**), and 7.1% (**2d**) is considerably larger. This leads to a strengthening and shortening of the Os–Si bond due to multiple bonding. The effect increases in the order Me < OH < Cl < F, and the Os–Si distances decrease in the same order. As discussed earlier, the Os–Si bond lengths are overestimated by 5–6 pm, and calculations with the geometry fixed at that observed by X-ray crystallography for **1a** showed increased delocalization from osmium to silicon (e.g., 7.2% for lp_i (Os) in **2a**) and decreased delocalization from osmium to the carbonyl group (e.g., 11.6% for lp_i (Os) in **2a**). Therefore, the SiF₃ group can be estimated to have almost half the π -acceptor ability of a carbonyl group. This is in good agreement with the results deduced from the photoelectron spectra on CpFe(SiCl₃)(CO)₂ for which the SiCl₃ group is estimated to have about half of the π -acceptor ability of a carbonyl group in this compound.

A comparison between the free silanes **3a–d** and the corresponding silyl complexes **2a–d** shows no significant changes of the d-orbital populations on silicon. Nonetheless, the d-orbitals serve to polarize the Si–R σ^* -orbitals in the transition metal complexes **2a–d** in such a way that this enhances the π -bonding between Si and Os and diminishes antibonding between Si and R (R = F, Cl, OH, and Me). Indeed, calculations without silicon d-orbitals show that they are important for a quantitative description of the bonding situation. Figure 3a shows no nodal plane between silicon and the in plane fluorine atom, whereas the nodal plane of the Si–F_i σ^* -orbitals is still present when neglecting the d-orbitals on silicon. Figure 4b depicts the important

polarization of a silicon p-orbital with 10.8% d-orbital contribution toward the osmium center. The d-orbital contribution to the orbital shown in Figure 3b is only 3.7%.

A second important result of the NLMO analysis is the high bond order between silicon and the carbon of the carbonyl group. This parameter increases from 0.10 to 0.11, 0.14, and 0.16 when going from **2d** to **2c**, **2b**, and **2a** and correlates directly with the observed stretching frequencies of the carbonyl groups. This interaction is consistent with the very small Si–Os–C(O) angle found for **2a–d**. The ν (CO) values for these compounds could, therefore, be influenced by a direct interaction between the silyl groups and the CO ligands as well as the electron-withdrawing or π -accepting nature of the silyl group reducing the electron density at the osmium center. There is precedent for Si–CO interactions in the compound Cp₂Zr(η^2 -Me₂Si=NBu)(CO).¹⁹

The harmonic vibrational analyses were not in good agreement with the experimentally obtained data, which is a common feature when modeling large molecules at a relatively moderate level of theory. Nevertheless, the calculated higher frequencies of 1834 and 1836 cm⁻¹ for the trifluoro and trichloro complexes respectively, and lower values of 1793 and 1800 cm⁻¹ for the trihydroxy and trimethyl derivatives show some acceptable agreement with the experimentally obtained values.

Conclusions

The acquisition of X-ray structural data for a set of five-coordinate osmium–silyl complexes with the silyl ligand changing from SiF₃ to SiCl₃ to Si(OH)₃ to SiMe₃ provided the opportunity to study the influence of a wide range of different SiR₃ groups on the nature of the osmium–silicon bond. Besides a likely strengthening of the Os–Si σ -bond due to ionic contributions only, *ab initio* calculations and subsequent NBO analyses revealed an increasing importance of π -bonding when going from the methyl to the hydroxy, the chloro, and finally the fluoro derivative. The group with the highest electronegativity, SiF₃, was estimated to have almost half the π -acceptor ability of the carbonyl group in the same molecule. No higher d-orbital population on silicon was found in any complex when compared with the corresponding free silanes, and the osmium d-orbitals mostly donate into a linear combination of Si–R σ^* -orbitals to form the π -bond. Nonetheless, d-orbitals on silicon are important in the quantitative description of the Os–Si bond as they serve to polarize the Si–R σ^* -orbitals, and this not only enhances the π -bonding between osmium and silicon but also diminishes the antibonding between Si and F, Cl, OH, and Me. The CO stretching frequencies were found to increase in the order Me to OH, Cl, and F. This is commonly explained with a diminished electron density at the osmium center if more electronegative groups are introduced into the complex. Population analyses on the set of five-coordinate osmium–silyl complexes show that this effect is also due to a direct influence of the silyl ligand on the carbonyl group in terms of a three-center bond

(19) Procopio, L. J.; Carroll, P. J.; Berry, D. H. *Polyhedron* **1995**, *14*, 45.

between osmium, silicon, and the carbon of the CO group which decreases in the order $F > Cl > OH > Me$.

Experimental Section

General Methods. All reactions were carried out using standard Schlenk techniques in a dry atmosphere of oxygen-free dinitrogen. The solvents were carefully dried and distilled from the appropriate drying agents prior to use.²⁰ NMR spectra were measured at 25 °C on either a Bruker AM 400 or a DRX 400 spectrometer at 400.128 (¹H), 100.625 (¹³C), 376.478 (¹⁹F), 79.495 (²⁹Si), and 161.976 MHz (³¹P). All chemical shifts were recorded in ppm downfield from tetramethylsilane (¹H, ¹³C, ²⁹Si), fluorotrichloromethane (¹⁹F), or phosphoric acid (³¹P) on the δ scale. The carbon phosphorus coupling $^nJ_{CP}$ in the triphenylphosphine ligand stands for $|^nJ_{CP} + ^mJ_{CP}|$. Infrared spectra were recorded on a Digilab FTS-7 infrared spectrometer. Melting points are reported in degrees Celsius (uncorrected). Analytical data were obtained from the Microanalytical Laboratory, University of Otago. The compounds OsPhCl(CO)(PPh₃)₂,⁴ OsHCl(CO)(PPh₃)₃,²¹ and Os[Si(OH)₃]Cl(CO)(PPh₃)₂⁶ were all prepared according to literature procedures.

Computational Methods. All calculations were performed with the GAUSSIAN94^{22,31} program series. The density functional method applying Beckes 1988 gradient-corrected exchange functional²³ and the correlation functional of Lee, Yang, and Parr (BLYP) was applied.²⁴ Structures were fully optimized at all levels of theory using gradient techniques. Stationary points were confirmed by frequency analysis. Effective core potentials were used to represent the 60 innermost electrons of the osmium atom,²⁵ as well as the 10-electron core of the silicon and phosphorus atoms.²⁶ The valence double- ζ basis sets with a (341/321/21) contraction for osmium and a (21/21) contraction for silicon, phosphorus, and chlorine were those associated with the pseudopotentials (LANL2DZ basis set²²), supplemented with a polarization of the d-shell for silicon.²⁷ Carbon, oxygen, and fluorine atoms were described by Dunning/Huzinaga double- ζ basis sets using a (721/41) contraction.²⁸ For the hydrogen atoms, a set of (31) contracted basis functions²⁹ were used. These basis set limitations were necessary due to the large computer time and disk space requirements for the DFT calculations. Although the resulting optimized complexes showed almost perfect C_s symmetry, the optimizations were carried out without any

symmetry restrictions starting from different geometries including the coordinates obtained from the X-ray analyses. To study the bonding situation in more detail, the natural localized molecular orbitals (NLMOs)³⁰ based on natural bond orbital (NBO)³¹ analyses were computed for all geometry-optimized structures by the following procedure. First, two-center, two-electron bonds were calculated for all model complexes with two double bonds from the carbon atom of the carbonyl group to both osmium and oxygen. The set of NBOs automatically found by the NBO program for the free silanes include one H–Si bond and three single bonds between silicon and the three R groups. In the second step, the systems were allowed to delocalize.

Os(SiF₃)Cl(CO)(PPh₃)₂ (1a). Os[Si(OH)₃]Cl(CO)(PPh₃)₂ (0.100 g, 0.117 mmol) was dissolved in dichloromethane (5 mL) and ethanol (5 mL). Aqueous HF (40%) (2 mL) was added, and the solution was stirred vigorously for 20 min. After ethanol (20 mL) was added, the yellow product was collected by filtration and washed well with ethanol–water–ethanol. Recrystallisation from CH₂Cl₂/ethanol gave pure **1a** (0.094 g, 93%). Mp 221–226 °C; ¹H NMR (CDCl₃) δ 7.60–7.36 (m, 30H, P(C₆H₅)₃); ¹³C NMR (CDCl₃) δ 179.2 (t, ²J_{CP} = 8.6 Hz, CO), 134.4 (t', ^{2/4}J_{CP} = 5.5 Hz; *o*-C₆H₅), 130.7 (t', ^{1/3}J_{CP} = 26.2 Hz, *i*-C₆H₅), 130.7 (s, *p*-C₆H₅), 128.5 (t', ^{3/5}J_{CP} = 5.0 Hz, *m*-C₆H₅); ²⁹Si NMR (CH₂Cl₂/CDCl₃) δ -74.3 (qt, ²J_{SiP} = 16.3, ¹J_{SiF} = 333.7 Hz); ¹⁹F NMR (CDCl₃) δ -89.64 (s); IR (Nujol) ν 1954 (CO), 1931 (CO), 880 (SiF), 866 (SiF), 820 (SiF); solution IR (CH₂Cl₂) 1946 (CO). Anal. Calcd for C₃₇H₃₀ClF₃OP₂SiOs (863.32): C, 51.48; H, 3.50. Found: C, 51.10; H, 3.98.

Os(SiCl₃)Cl(CO)(PPh₃)₂ (1b). (a) HSiCl₃ (0.470 g, 3.5 mmol) was introduced to a solution of OsPhCl(CO)(PPh₃)₂ (0.200 g, 0.23 mmol) in dry toluene (10 mL) in a Schlenk tube, which was then sealed. The solution was heated at 40 °C with stirring for 30 min. The yellow solution was evaporated to a small volume *in vacuo*, and then dry *n*-hexane was added to effect crystallization of **1b** (0.188 g, 88%). (b) HSiCl₃ (0.530 g, 4.0 mmol) was added to a solution of OsHCl(CO)(PPh₃)₃ (0.200 g, 0.19 mmol) in dry toluene (10 mL) in a Schlenk tube, which was then sealed. The solution was heated to 60 °C with stirring for 20 min. Pure, yellow crystals of **1b** were afforded by reduction of the volume of the solution *in vacuo*, and then dry *n*-hexane was added (0.165 g, 94%). Mp 200–203 °C; ¹H NMR (CDCl₃) δ 7.75–7.30 (m, 30H; P(C₆H₅)₃); ¹³C NMR (CDCl₃, with Cr(acac)₃ as a relaxation reagent): δ 179.6 (t, ²J_{CP} = 8.5 Hz, CO), 134.7 (t', ^{2/4}J_{CP} = 5.1 Hz, *o*-C₆H₅), 130.7 (s, *p*-C₆H₅), 130.0 (t', ^{1/3}J_{CP} = 26.2 Hz, *i*-C₆H₅), 128.3 (t', ^{3/5}J_{CP} = 4.7 Hz; *m*-C₆H₅); ³¹P NMR (CH₂Cl₂/CDCl₃) 22.7 (s); IR (Nujol) ν 1944 (CO). Anal. Calcd for C₃₇H₃₀Cl₄OSiP₂Os (912.69): C, 48.69; H, 3.31. Found: C, 48.71; H, 3.26.

Os(SiMe₃)Cl(CO)(PPh₃)₂ (1d). MeLi (0.009 g, 0.43 mmol) in diethyl ether was added to Os(SiCl₃)Cl(CO)(PPh₃)₂ (0.120 g, 0.13 mmol) in dry toluene (5 mL) with stirring at room temperature. Immediately, the color of the solution changed from yellow to red-orange. The solution was stirred for several minutes before the volume of the solvent was reduced by half *in vacuo*. The solution was then placed on a flash column with a silica gel support and chromatographed using an eluent of toluene/*n*-hexane (80:20). The yellow-orange band eluted first from the column was collected, and the solvent was removed under reduced pressure. Recrystallization of the residual solid using CH₂Cl₂/*n*-hexane yielded yellow-orange crystals of pure **1d** (0.040 g, 36%). Mp 181–182 °C; ¹H NMR (CDCl₃) δ 7.60–7.34 (m, 30H, P(C₆H₅)₃), 0.14 (s, 9H, Si(CH₃)₃); ¹³C NMR (CDCl₃) δ 183.2 (t, ²J_{CP} = 8.1 Hz, CO), 134.6 (t', ^{2/4}J_{CP} = 4.9 Hz, *o*-C₆H₅), 132.4 (t', ^{1/3}J_{CP} = 24.5 Hz, *i*-C₆H₅), 130.0 (s, *p*-C₆H₅), 128.0 (t', ^{3/5}J_{CP} = 4.5 Hz, *m*-C₆H₅), 9.1 (s, Si(CH₃)₃); ³¹P NMR (CH₂Cl₂/CDCl₃) δ 21.9 (s); IR (Nujol) ν 1910 (CO), 1888 (CO), 835 (SiC); solution IR (CH₂Cl₂) ν 1895 (CO). Anal. Calcd for C₄₀H₃₉ClOP₂SiOs (851.43): C, 56.43; H, 4.62. Found: C, 56.92; H, 5.11.

X-ray Experimental Data for 1a, 1b-CH₂Cl₂, and 1d. Data were collected on an Enraf-Nonius CAD4 diffractometer.

(20) Perrin, D. D.; Armarego, W. L. F. *Purification of Laboratory Chemicals*, 3rd ed.; Pergamon Press: New York, 1988.

(21) Vaska, L. *J. Am. Chem. Soc.* **1964**, *86*, 1943.

(22) Frisch, M. J.; Trucks, G. W.; Schlegel, H. B.; Gill, P. M. W.; Johnson, B. G.; Robb, M. A.; Cheeseman, J. R.; Keith, T.; Petersson, G. A.; Montgomery, J. A.; Raghavachari, K.; Al-Laham, M. A.; Zakrzewski, V. G.; Ortiz, J. V.; Foresman, J. B.; Cioslowski, J.; Stefanov, B. B.; Nanayakkara, A.; Challacombe, M.; Peng, C. Y.; Ayala, P. Y.; Chen, W.; Wong, M. W.; Andres, J. L.; Replogle, E. S.; Gomperts, R.; Martin, R. L.; Fox, D. J.; Binkley, J. S.; Defrees, D. J.; Baker, J.; Stewart, J. P.; Head-Gordon, M.; Gonzalez, C.; Pople, J. A. *Gaussian 94*, Revision D.3, Gaussian, Inc.: Pittsburgh, PA, 1995.

(23) Becke, A. D. *Phys. Rev.* **1988**, *A38*, 3098.

(24) Lee, C.; Yang, W.; Parr, R. G. *Phys. Rev.* **1988**, *B37*, 785. Miehlich, B.; Savin, A.; Stoll, H.; Preuss, H. *Chem. Phys. Lett.* **1989**, *157*, 200.

(25) Hay, P. J.; Wadt, W. R. *J. Chem. Phys.* **1985**, *82*, 299.

(26) Wadt, W. R.; Hay, P. J. *J. Chem. Phys.* **1985**, *82*, 284.

(27) Franch, M. M.; Pietro, W. J.; Hehre, W. J.; Binkley, J. S.; Gordon, M. S.; DeFrees, D. J.; Pople, J. A. *J. Chem. Phys.* **1982**, *77*, 3654.

(28) Dunning, T. H., Jr.; Hay, P. J. In *Modern Theoretical Chemistry*; Schaefer, H. F., Ed.; Plenum: New York 1976; pp 1ff.

(29) Ditchfield, R.; Hehre, W. J.; Pople, J. A. *J. Chem. Phys.* **1971**, *54*, 724. Hehre, W. J.; Ditchfield, R.; Pople, J. A. *Ibid* **1972**, *56*, 2257. Hariharan, P. C.; Pople, J. A. *Mol. Phys.* **1974**, *27*, 209. Gordon, M. S. *Chem. Phys. Lett.* **1980**, *76*, 163. Hariharan, P. C.; Pople, J. A. *Theor. Chim. Acta* **1973**, *28*, 213.

(30) Reed, A. E.; Weinhold, F. *J. Chem. Phys.* **1985**, *83*, 1736. Reed, A. E.; Schleyer, P. v. R. *J. Am. Chem. Soc.* **1990**, *112*, 1434.

(31) Glendening, E. D.; Reed, A. E.; Carpenter, J. E.; Weinhold, F. *NBO*, Version 3.1; part of Gaussian 94, Revision D.3; Gaussian, Inc., Pittsburgh, PA, 1995.

An empirical absorption correction was applied. The structure was solved by Patterson methods, and refinement on F^2 was carried out by full-matrix least-squares techniques (SHELXL93).³² Anisotropic temperature factors were used for all non-hydrogen atoms except for the water molecule. Hydrogen atoms were included in calculated positions with isotropic temperature factors 20% higher than the corresponding carbon atoms. Further results of the refinement are listed in Table 2.

(32) Sheldrick, G. M. *SHELXL93*; University of Göttingen, Göttingen, Germany, 1993.

(33) Schaftenaar, G. *MOLDEN 3.2*, CAOS/CAMM Center: The Netherlands, 1996.

Acknowledgment. We thank the Alexander von Humboldt-Stiftung for the award of a Feodor-Lynen scholarship to K.H. X-ray data for compound **1d** was generously provided by G. R. Clark. Support from the AURC (Auckland) is gratefully acknowledged.

Supporting Information Available: Tables of atomic coordinates, thermal parameters, and interatomic distances and angles for **1a** and **1d** (19 pages). Ordering information is given on any current masthead page.

OM970580H